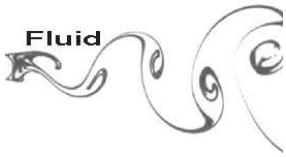

FLUid Image analysis and Description (FLUID)
Project No. FP6-513663
FET - Open Domain, Priority IST

Second set of fluid mechanics image sequences

Johan Carlier[1]

Project cofunded by the European Comission
within the Sixth Framework Programme (2002-2006).

Dissemination level: PU (Public) Revision: 1

[1]Cemagref Team, johan.carlier@cemagref.fr

Contents

1 Analytic flows

In the first package, one set of images from analytic flows has already been delivered. In this second package, a new set are delivered with more little displacements and image size.

1.1 Viscous flow

In some simple viscous flows, it is possible to find the exact solution of the Navier-Stokes equations. Poiseuille and Lamb-Oseen Vortex flows are two well know examples with velocity gradients. Figure 1 presents the velocity fields for the viscous flows. Moreover, a third case with simple gradient in longitudinal velocity is added.

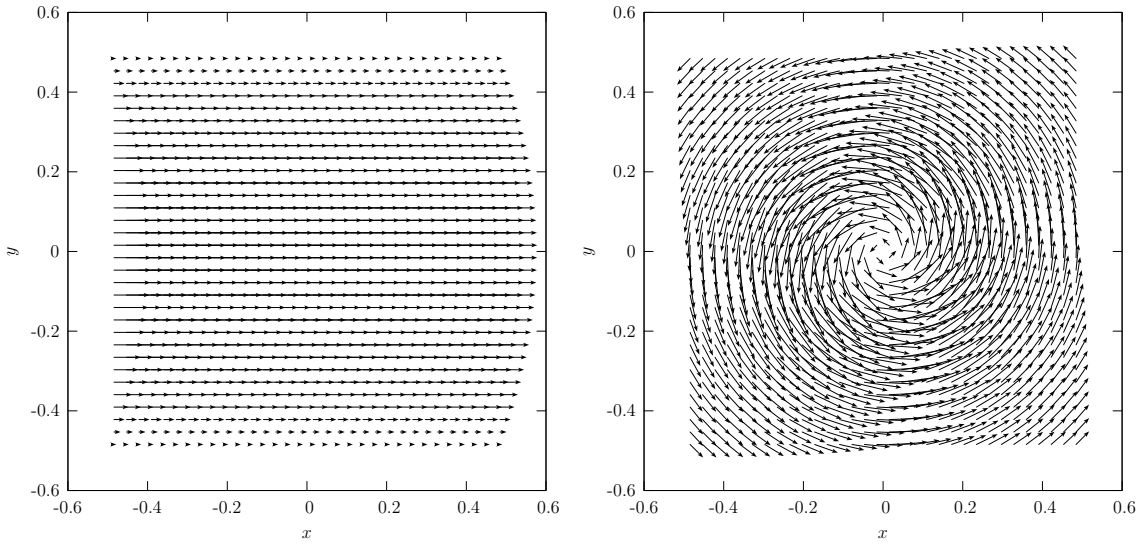

Poiseuille Lamb-Oseen

Figure 1: Velocity fields for the viscous flow

1.1.1 Simple gradient

The equation used for the simple gradient field is:

$$u_x = U\frac{y}{h} \quad (1)$$

$$u_y = 0 \quad (2)$$

$$u_z = 0 \quad (3)$$

with $U = 1/256\ \mathrm{m.\,s^{-1}}$, $h = 0.5$ m and $y \in [-0.5, +0.5]$ m

1.1.2 Poiseuille Flow

The Poiseuille flow is a viscous flow between two parallel plates with a constant streamwise pressure gradient. The plates are located at the bottom and the top borders of the image. The equation for the permanent velocity field is:

$$u_x = U\left(1 - \frac{y^2}{h^2}\right) \tag{4}$$

$$u_y = 0 \tag{5}$$

$$u_z = 0 \tag{6}$$

with $U = 1/128\ \mathrm{m.\,s^{-1}}$, $h = 0.5$ m and $y \in [-0.5, +0.5]$ m

1.1.3 Lamb-Oseen Vortex

The Lamb-Oseen vortex is a two-dimensional viscous flow with circular streamlines and a decreasing vorticity along the radial distance r and the time t. The exact solution of the Navier-Stokes equations is:

$$u_\theta(r, \theta, t) = \frac{\Gamma_0}{2\pi r}\left(1 - e^{-r^2/4\nu t}\right) \tag{7}$$

where ν is the cinematic viscosity and Γ_0 is the initial circulation. In the present work, $\Gamma_0 = 0.005\ \mathrm{m^2.\,s^{-1}}$ and t is fixed with $4\nu t = (1/6)^2\ \mathrm{m^2}$ ($\sqrt{4\nu t}$ can be seen as the radius of the Lamb-Oseen Vortex).

1.2 Potential flows

In a $2D$ incompressible ($\boldsymbol{\nabla} \cdot \boldsymbol{u} = 0$), irrotational fluid flow ($\boldsymbol{\nabla} \wedge \boldsymbol{u} = \boldsymbol{0}$), it is possible to introduce an analytic function of the complex variable $z = x + iy$ for which the real and imaginary parts correspond to the velocity potential and the stream function:

$$f(z) = \phi(z) + i\psi(z) \tag{8}$$

The components of the velocity can be derived from the stream function derivatives:

- in cartesian coordinates:

$$u_x = +\frac{\partial \psi}{\partial y} \tag{9}$$

$$u_y = -\frac{\partial \psi}{\partial x} \tag{10}$$

- in polar coordinates:

$$u_r = +\frac{1}{r}\frac{\partial \psi}{\partial \theta} \tag{11}$$

$$u_\theta = -\frac{\partial \psi}{\partial r} \tag{12}$$

The potential flow provided are an uniform flow, a sink, a vortex and a potential flow around a cylinder with circulation. Their corresponding velocity field solutions are presented on figure 2.

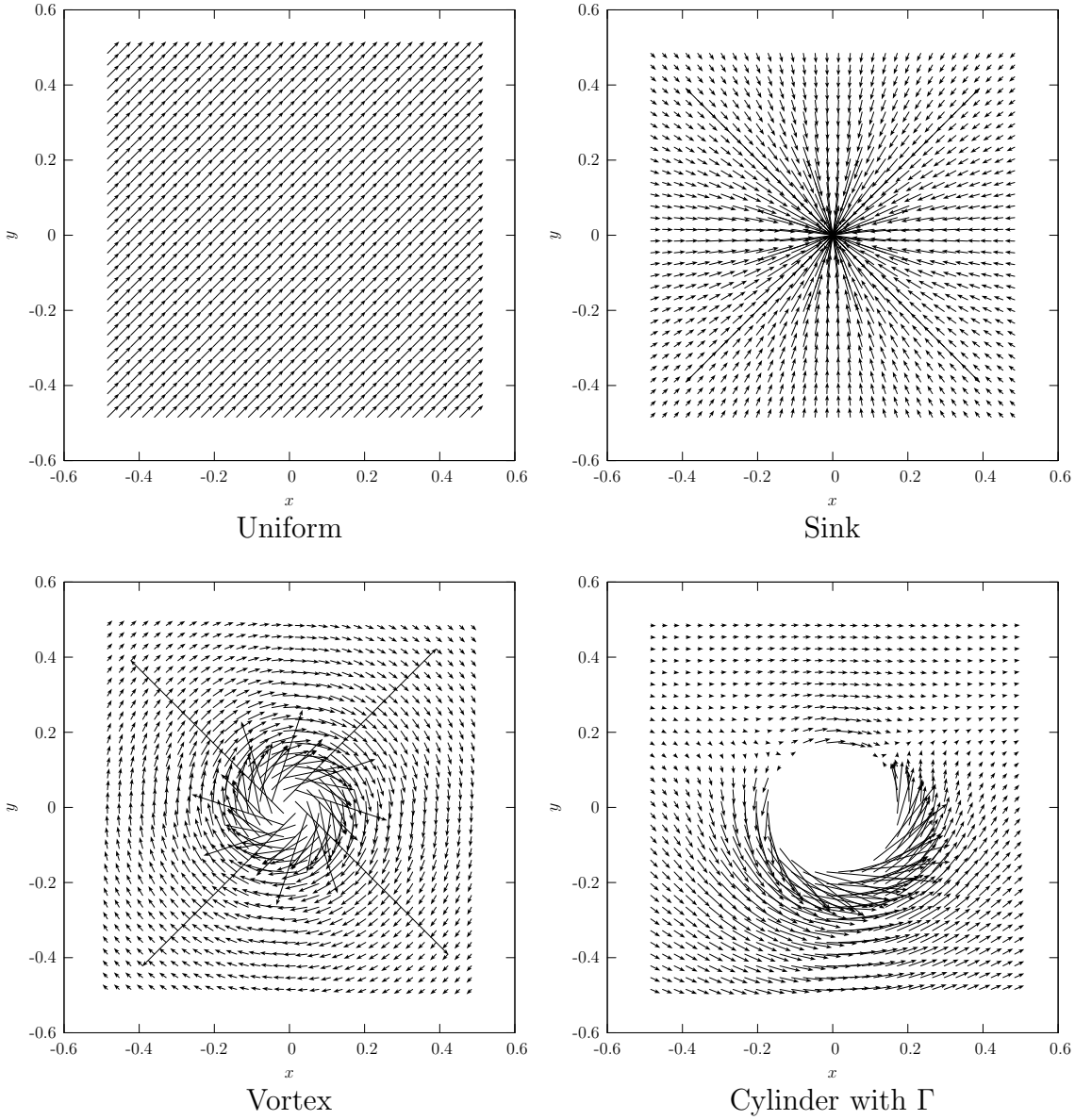

Figure 2: Velocity fields for the potential flows

1.2.1 Uniform flow

An uniform flow can be seen as a potential flow. The analytic function of the complex variable for a such flow is:

$$f(z) = Uz \tag{13}$$

with $U = 1/256$ m. s^{-1} in our case. However, it is more convenient to write the equation for the displacement field between successive images as:

$$\Delta x = 1 \text{ px} \tag{14}$$

$$\Delta y = 1 \text{ px} \tag{15}$$

$$\Delta z = 0 \text{ px} \tag{16}$$

1.2.2 Sink flow

The analytic function of the complex variable is:

$$f(z) = \frac{D}{2\pi} \log z \tag{17}$$

The imaginary part is the stream fonction with:

$$\psi = \frac{D}{2\pi}\theta \tag{18}$$

The stream fonction allows to get the velocity field in polar coordinates with:

$$u_r = \frac{\partial r}{\partial t} = \frac{D}{2\pi r} \tag{19}$$

$$u_\theta = \frac{1}{r}\frac{\partial \theta}{\partial t} = 0 \tag{20}$$

This system of Ordinary Differential Equations can be integrated easily to get the lagrangian representation of the particle coordinate evolutions:

$$r^2 = r_0^2 + \frac{D}{2\pi}(t - t_0) \tag{21}$$

$$\theta = \theta_0 \tag{22}$$

with the flow rate $D = -0.001$ m^2. s^{-1} in the provided case.

1.2.3 Vortex flow

The analytic function of the complex variable is:

$$f(z) = -i\frac{\Gamma}{2\pi} \log z \tag{23}$$

The imaginary part is the stream fonction with:

$$\psi = -\frac{\Gamma}{2\pi}\log r \tag{24}$$

The stream fonction allows to get the velocity field in polar coordinates with:

$$u_r = \frac{\partial r}{\partial t} = 0 \tag{25}$$

$$u_\theta = \frac{1}{r}\frac{\partial \theta}{\partial t} = \frac{\Gamma}{2\pi r} \tag{26}$$

The evolution of particle coordinates is:

$$r = r_0 \tag{27}$$

$$\theta = \theta_0 + \frac{\Gamma}{2\pi r} \tag{28}$$

with the circulation $\Gamma = -0.001\ \mathrm{m}^2.\mathrm{s}^{-1}$ in the provided case.

1.2.4 Potential flow around a cylinder with circulation

This flow is the superposition of a uniform flow, a doublet (not defined here) and a vortex. The analytic function of the complex variable is:

$$f(z) = Uz - i\frac{\Gamma}{2\pi}\log z + \frac{K}{2\pi z} \tag{29}$$

The corresponding system of Ordinary Differential Equations is:

$$\frac{\partial r}{\partial t} = +U\left(1 - \frac{R^2}{r^2}\right)\cos\theta + 0. \tag{30}$$

$$\frac{\partial \theta}{\partial t} = -\frac{U}{r}\left(1 + \frac{R^2}{r^2}\right)\sin\theta + \frac{\Gamma}{2\pi r^2} \tag{31}$$

This system was integrated by a Runge-Kutta algorithm with $U = 1/256\ \mathrm{m}.\mathrm{s}^{-1}$, $R = 1/6$ m, $\beta = \pi/4$, $K = 2\pi R^2 U$ and $\Gamma = 4\pi R U \sin\beta$. U is the external velocity, R the radius of the cylinder and β the angle defining the positions of the two stagnation points in the cylinder.

1.3 Set of images delivered

For each of those analytic flows, 41 successive images are given in TIF-format with 8 bits in depth. The same parameters (particle size, concentration, intensity, *etc*) are used for all the initial images as summarized below:

Width of the image (in pixel):	512
Height of the image (in pixel):	512
Width of the image (in meter):	1.
Height of the image (in meter):	1.
Time interval between shoots (in second):	1.
Thickness of the laser sheet (in meter):	.001
Width of the window (in pixel):	32
Height of the window (in pixel):	32
Number of particles per window (integer):	256
Diameter and deviation of the particle images (in pixel):	1.5 .25
Minimum grey-level in the image (integer):	16
Light scattering at the center (integer):	64

One sequence describes the trajectory of the particles along 41 timesteps, the trajectory being time independant here. Different computations are possible like analysing a sequence in sequential mode (0-1;1-2;2-3...), analysing a sequence with a stride (0-2;1-3;2-4...) in order to increase the displacements, or reversing a sequence in order to change the velocity sign (*i.e.* change the rotation of a vortex for exemple).

Case n°	Description	Directory
A1b	Poiseuille	USB-HDD ./package_02/analytic/
A2b	Lamb-Oseen vortex	USB-HDD ./package_02/analytic/
A3b	Uniform flow	USB-HDD ./package_02/analytic/
A4b	Sink flow	USB-HDD ./package_02/analytic/
A5b	Vortex flow	USB-HDD ./package_02/analytic/
A6b	Cylinder with circulation	USB-HDD ./package_02/analytic/

Table 1: Table location, Annexe A.3

The corresponding sequences were placed into the folders "package_02/analytic/" (see Tab. 1) and are named:

Uniform: "i01[01-41].tif" for the images and "i01_sol.txt" for the solution

gradient: "i02[01-41].tif" for the images and "i02_sol.txt" for the solution

Poiseuille: "i03[01-41].tif" for the images and "i03_sol.txt" for the solution

Lamb-Oseen: "i04[01-41].tif" for the images and "i04_sol.txt" for the solution

Sink: "i05[01-41].tif" for the images and "i05_sol.txt" for the solution

Vortex: “i06[01-41].tif” for the images and “i06_sol.txt” for the solution

Cylinder: “i07[01-41].tif” for the images and “i07_sol.txt” for the solution

2 Wake behind a circular cylinder

2.1 Experiment

This section describes a $2D$-$2C$ PIV experiment carried out in one of the wind tunnels of the Rennes Regional Centre of Cemagref.

2.1.1 Wind tunnel

The sketch (in front view) of the wind tunnel used in this experiment is presented in Fig. 3. The aeraulic circuit is mainly made of a centrifugal fan, a diffuser, a plenum chamber with honey comb and grids, a convergent with a contraction coefficient of 4 and a testing zone with transparent walls. The testing zone is squared in cross section with 280 mm of with dimensions and 100 cm in length. The upper wall is slightly tilted to suppress the longitudinal pressure gradient. The flow velocity can be chosen continuously between 1 and 8 $\mathrm{m.\,s^{-1}}$ with a good stability. The uniformity of the velocity profile at the entrance of test section was checked by hot-wire anemometry. The free stream turbulence intensity was less than 0.5%. The temperature was kept within $\pm 0.2^\circ$ C by using an air-water heat-exchanger.

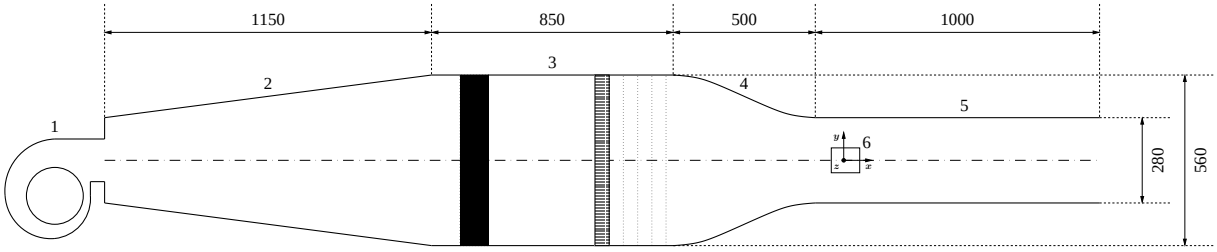

1 : Centrifugal fan
2 : Low divergent section
3 : Plenum chamber
4 : Contraction section
5 : Testing section
6 : Cylinder and end-plates

Figure 3: Front view of the windtunnel.

The circular cylinder has a length $L = 280$ mm and a diameter $D = 12$ mm. It is equipped with 2 thin rectangular end plates. The distance between the end-plates is 240 mm providing an aspect ratio $L/D = 20$. The clearence between the walls and the

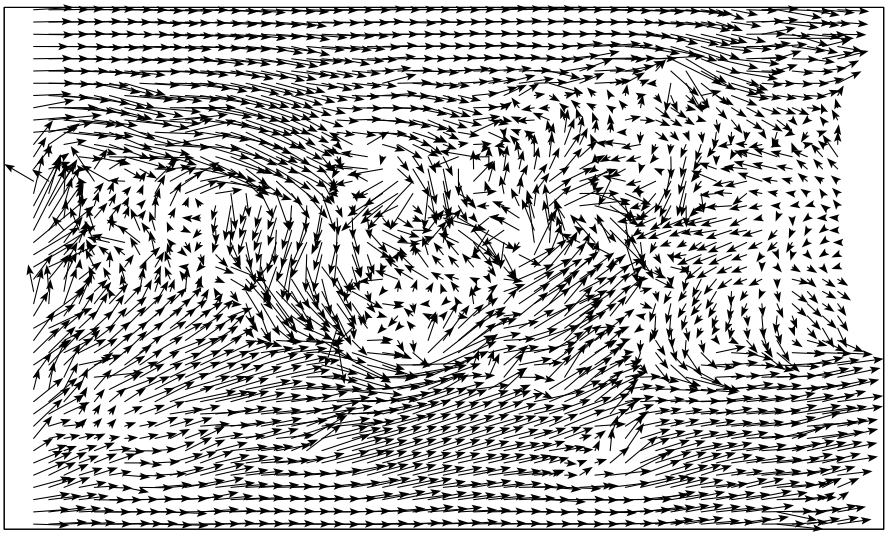

Figure 4: Structure of the velocity fields (a constant velocity component u has been subtracted)

end-plates is about 20 mm which is much larger than the thickness of the boundary layer on the wall. The blockage ratio is 4.3%. The circular cylinder is mounted horizontaly at $3.5D$ from the entrance of the testing zone.

The reference frame is direct and the origin is located at the center of the cylinder. The longitudinal x-axis is the testing zone axis of the wind tunnel, y-axis is normal to the wake central plane (symmetry plane) and z-axis is the cylinder axis. u, v and w are the velocity components related to x, y and z axis respectively.

2.1.2 Measurements

$2D$-$2C$ PIV experiments (2 in-plane velocity components in a plane field) were carried out with NewWave Solo 3 Nd-YAG laser (Energy by pulse of 50 mJ) and a SensiCam PCO cameras (CCD size of 1280×1024 px^2 and dynamics of 12 bits). The laser sheet was produced by means of a Rodenstock telescope and a cylindrical lens. The diameter of the particle seeding (diluted polyglycol in water) is less than 10 μm. The measurement area was located $30D$ behind the circular cylinder, in the plane $z = 0$. The camera was located perpendicularly to the laser sheet at a distance of 100 cm. For the mounted lens, the focal length was 105 mm with an aperture of 5.6. The resulting field of view is about $8D \times 6.4D$. The free-stream velocity was adjusted at 4.8 m. s^{-1} so that the Reynolds number Re_D be 3 900 (Reynolds number based on the free stream velocity Ue, the cinematic viscosity ν and the diameter of the circular cylinder D). 5 000 image pairs

were obtained with a time interval of 200 μs. To give an idea of the flow structure, Fig. 4 shows a modified velocity field where a constant velocity component has been substracted (calculated with a classical PIV algorithm).

2.1.3 Set of images delivered

5 000 image pairs were delivered in TIF-format with 16 bits in depth[2]. The exact image size is 96.38 mm in length (1 280 px) and 77.03 mm in height (1 024 px). The location of the lower left corner of the image is $x = 319.62$ mm and $y = -38.40$ mm. The 5 000 image pairs are located in "package_02/exp_wake/image/" (see Tab. 2). "a0[0001-5000]a.tif" are the first images in pairs and "a0[0001-5000]b.tif" are the second.

Case n°	Description	Directory
D1	Exp. far wake	USB-HDD ./package_02/exp_wake/

Table 2: Table location, Annexe A.3

2.2 Large Eddy Simulation

2.2.1 General description of the code

The code[3] used for this study solved the incompressible Navier-Stokes equations:

$$\frac{\partial u_i}{\partial t} + \frac{\partial u_i u_j}{\partial x_j} = -\frac{1}{\rho_0}\frac{\partial p_m}{\partial x_i} + \nu\frac{\partial^2 u_i}{\partial x_j \partial x_j} + f_i, \tag{32}$$

$$\frac{\partial u_i}{\partial x_i} = 0, \tag{33}$$

where ν is the (constant) kinematic viscosity, ρ_0 the (constant) density, p_m the modified pressure field. f_i is a force which mimics the effects of a solid obstacle in the flow. Basically, Large Eddy Simulation method consists in separating, from a spatial filtering operation, the great scales and the small scales of the turbulence. Spatial filtering (denoted by the overbar) of the Navier-Stokes equations is:

$$\frac{\partial \bar{u}_i}{\partial t} + \frac{\partial \bar{u}_i \bar{u}_j}{\partial x_j} = -\frac{1}{\rho_0}\frac{\partial \bar{p}_m}{\partial x_i} + \nu\frac{\partial^2 \bar{u}_i}{\partial x_j \partial x_j} + \bar{f}_i + \frac{\partial T_{ij}}{\partial x_j}, \tag{34}$$

[2]With classical viewer, the images may appear relatively black and seem to be poorly enlighted. In fact, the original images are 12 bits in depth and are converted for more convenience in TIF-format with 16 bits in depth, giving artificially low values as compared to the global 16 bits range.

[3]Reference: P. Parnaudeau, PhD thesis, *Étude num´rique d'un écoulement cisaillé turbulent complexe basse vitesse : Application à la protection rapprochée*

$$\frac{\partial \bar{u}_i}{\partial x_i} = 0, \tag{35}$$

where $T_{ij} = \bar{u}_i\bar{u}_j - u_i\bar{u}_j$ is the subgrid-scale stress. According to the Boussinesq hypothesis, the subgrid-scale stress can be defined as:

$$T_{ij} = \nu_t\left(\frac{\partial \bar{u}_i}{\partial x_j} + \frac{\partial \bar{u}_j}{\partial x_i}\right) + \frac{1}{3}T_{kk}\delta_{ij}. \tag{36}$$

where ν_t is evaluated by the Function Structure model. Here, $\nu_t \sim \Delta_c\nu_\Delta$, where Δ_c is the filter width and ν_Δ the subfilter length scale. According to Deardorff $\Delta_c = (\Delta_x\Delta_y\Delta_z)^{1/3}$, where Δ_x,Δ_y, Δ_z, are the filter widths in each direction.

The incompressible Navier-Stokes equations are solved on a regular Cartesian grid in non-staggered configuration. Sixth-order compact centered difference schemes are used to evaluate all spatial derivatives, except at the outlet and outflow boundaries where single sided schemes were employed for the x-derivative calculation. Time integration is performed with the second-order Adams-Bashforth scheme. A constant flow is imposed at the entrance of the domain and a simple convection equation is applied at the exit. Periodic conditions are used in the two transverse direction y and z.

Our computational domain extends over $20D$ in the streamwise and normal directions. The center of the cylinder is located at $x_{cyl} = 5D$ downstream of the inflow. The spanwize extent of the domain was chosen to be $L_z = \pi D$, which corresponds to the size used by most previous authors. For the square which contains the cylinder, we only used 48×48 points in the streamwise and normal directions. A uniform streamwize flow is imposed in the initial conditions, with no perturbation in the other directions. For the regime considered, the boundary layer is laminar. The simulation was carried out with a constant time step size of $\Delta t = 0.003D/U_c$ which ensured that the Courant number be 0.15. The Reynolds number is $Re_D = 3\,900$, the domain size is $L_x \times L_y \times L_z = 20D \times 20D \times \pi D$ and the corresponding number of point is $n_x \times n_y \times n_z = 961 \times 960 \times 48$. Fig. 5 presents the iso-surface of the vorticity norm near the cylinder.

2.2.2 Set of images delivered

200 full $3D$ velocity fields with a $20\Delta t$ time step between them are available for the post-processing. Particles are randomly distributed in the $3D$ domain. For each particle, the Lagrangian equation for non-heavy particle is solved:

$$\frac{d\boldsymbol{x}\,(x,t)}{dt} = \boldsymbol{u}\,(x,t) \tag{37}$$

For this package, the turbulent wake flow is frozen to make easier the resolution of the Lagrangian equation. Then, $\boldsymbol{u}\,(x,t)$ becomes $\boldsymbol{u}\,(x)$ and only one $3D$ velocity field (for $t = t_0$) is used for the computation of a sequence of particle images.

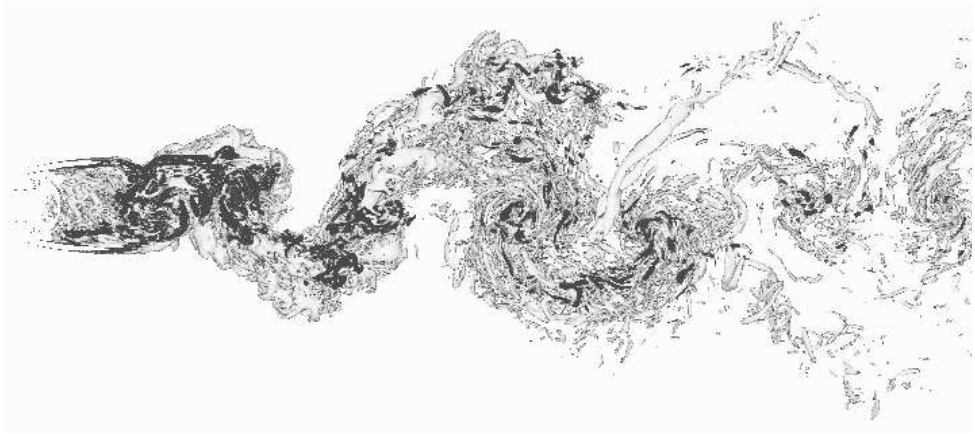

Figure 5: Iso-surface of the vorticity norm

Coordinates of all the particles are recorded every $10\Delta t$ during $90\Delta t$. Gaussian particle shape ($\exp^{-1/2(r/D)^2}$ with $D = 3/\left(8^{1/2}\right)$ vx) is used to convert the 10 resulting files into $3D$ raw particle images. The image size is $960 \times 960 \times 144$ vx^3 (corresponding to $20D \times 20D \times \pi D$ with $D = 1$ or 48 px) and voxels are coded with one byte per voxel. The voxels are ordered with the following sequence: increasing first x, then y and finally z without separation. The mean particle concentration is arbitrary chosen at $1/4^3$ particle per voxel.

The 10 files are located in "package_02/les_wake/" (see Tab. 3) and are named "fld_00[0-9].raw". "wakles001.dat" is the $3D$ velocity field solution (unformatted files with 4 bytes/velocity components and with 4 bytes header and trailer) ordered with first u (increasing first x, then y and finally z), v and finally w. In order to have nearly cubic voxel size, the voxel generated mesh (*i.e.* $960 \times 960 \times 144$) is different from the velocity mesh (*i.e.* $961 \times 960 \times 48$) from which it is derived, but both have the same total "physical" size (*i.e.* $20D \times 20D \times \pi D$).

Case n°	Description	Directory
E1	LES wake - Volume	USB-HDD ./package_02/les_wake/

Table 3: Table location, Annexe A.3

3 $2D$ turbulent flow

3.1 Experiment

3.1.1 Set-up

The experiment has been carried out by Marie Caroline Julien during her Phd Thesis. The phenomenon investigated is the spreading of a low diffusivity dye in a $2D$ turbulent flow, forced at a large scale.

The flow has been generated in a square horizontal PVC cell with 15×15 cm^2 of with dimensions. The bottom of the cell is made of a thin (1 mm) glass plate, below which permanent magnets, $5 \times 8 \times 4$ mm^3 in size, are placed. Their magnetization axis is vertical and they produce a magnetic field, 0.3 T in maximum amplitude, which decays over a typical length of 3 mm. In order to ensure a $2D$ flow, the cell is filled with two layers of NaCl solution, each one 3 mm thick, with different densities, $\rho_1 = 1\,030\ g \cdot l^{-1}$ and $\rho_2 = 1\,060\ g \cdot l^{-1}$, placed in a stable configuration, *i.e.*, the heavier underlying the lighter. The interaction of an electrical current driven across the cell with the magnetic field produces Laplace forces which drive the flow. The magnets are arranged in four triangular blocks, so that the energy is injected, in average, at a scale of 10 cm. The excitation is permanently maintened. In such conditions, the flow develops, after a short transcient state, a direct enstrophy cascade with Kolmogorov-Kraichnan scaling, $E(k) = k^{-5/3}$. The homogeneity and isotropy properties of the regime has been checked. The characteristic scale of the motion, L, defined from the maximum in the energy spectrum, is found to be 10 cm. The main dissipation in this system is provided by the friction exerted by the bottom wall on the fluid. It can be parametrized by adding a linear term in the $2D$ Navier-Stokes equations. This friction term, if large enough, provides the infra-red energy sink preventing the accumulation of energy in the lowest accessible mode. It can be varied by changing the total fluid depth but the range of allowed depths is not wide since it is clear that a large fluid depth would ruin the two-dimensionality assumption.

The passive scalar is a mixture of fluorescein and water, of density $\rho = 1\,002\ g \cdot l^{-1}$, and diffusivity $\kappa = 10^{-6} cm^2 \cdot s^{-1}$. The concentration field, illuminated by ultra-violet light, is visualized using a 512×512 px^2 CCD camera. The intensity is proportional to the dye concentration. The spatial resolution for the concentration field is 0.3 mm. The Peclet number $Pe = UL/\kappa$ (where U is a typical velocity of the flow roughly approximatively evaluated at 1 $cm \cdot s^{-1}$) is around 10^7, the Reynold number $Re = UL/\nu$ is around $2\,000/3$ and the Schmidt number $Sc = Pe/Re$ is around 15 000. To inject the dye, a dye blob is enclosed in a cylinder, 5 cm in diameter, in the upper layer, then the electrical current is

switched on, the transcient states is observed until it vanishes, and the cylinder is removed. In these experiments, the flow is statistically stationary, while the concentration field is in a freely decaying regime. Owing to the experimental conditions (large scale forcing for the flow, high Peclet numbers), the Batchelor regime may be expected to take place for the dissipation of the tracer. Fig. 6 shows two samples of the scalar images at different times.

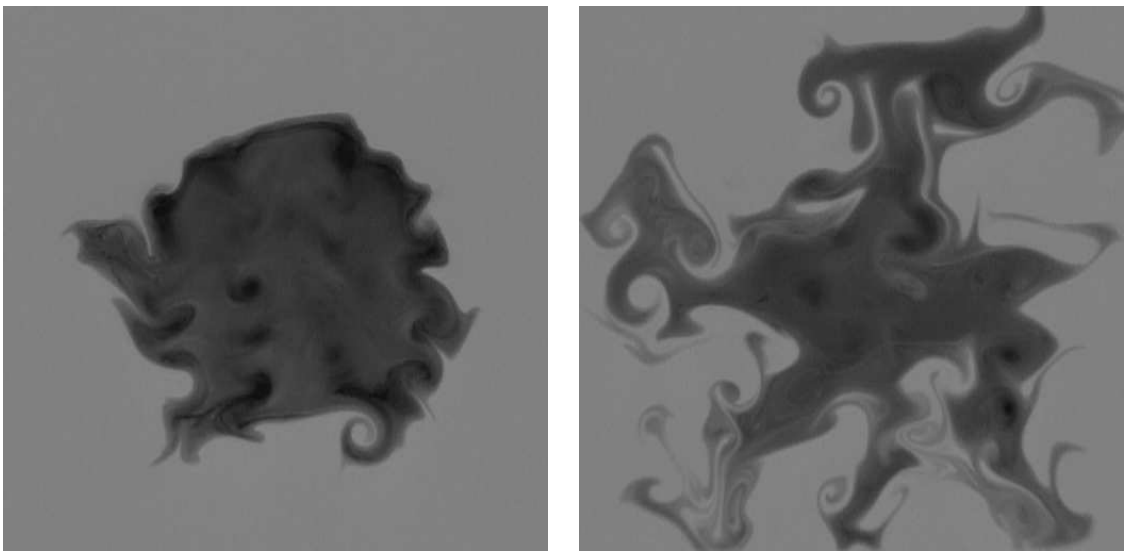

Figure 6: Two samples of the scalar images

3.1.2 Set of images delivered

The deliverable consists of 92 successive images showing the diffusion of a passive scalar in $2D$ turbulent flow. These images are located in "exp_tur2d/image/" (see Tab. 4) and are named "image[00-92].tif" (one byte tif-format). The image size is 15×15 cm^2 (512×512 px^2) of with dimensions and the time step between the images is on the order of 1 s.

Case n^o	Description	Directory
B	Exp. of 2D turbulent flow	USB-HDD ./package_02/exp_turb2d/

Table 4: Table location, Annexe A.3

3.2 Direct Numerical Simulation

The main interest of a synthetic image sequence database of numerically generated $2D$ turbulent flow fields is the knowledge of the exact solution along the time for flow with a

large scale range in the energy spectrum. For this purpose, DNS was perfomed to solve particle and scalar transport in $2D$ sustained turbulent flow.

3.2.1 General description of the code

The code[4] used for this study solved the Navier-Stokes equations:

$$\frac{\partial \boldsymbol{u}}{\partial t} + \boldsymbol{u} \cdot \boldsymbol{\nabla} \boldsymbol{u} = -\frac{1}{\rho} \boldsymbol{\nabla} p + \nu \boldsymbol{\nabla}^2 \boldsymbol{u} \tag{38}$$

with the incompressible condition:

$$\boldsymbol{\nabla} \cdot \boldsymbol{u} = 0, \tag{39}$$

the Lagrangian equation for non heavy particle transported by the flow:

$$\frac{d\boldsymbol{x}}{dt} = \boldsymbol{u} \tag{40}$$

and the advection-diffusion equation for a scalar transported by the flow:

$$\frac{\partial \Theta}{\partial t} + \boldsymbol{u} \cdot \boldsymbol{\nabla} \Theta = \kappa \boldsymbol{\nabla}^2 \Theta \tag{41}$$

By applying the $\boldsymbol{\nabla}$ operator to the Navier-Stokes equations in $2D$, the conservation equation for the vorticity ω is obtained:

$$\frac{\partial \omega}{\partial t} + \boldsymbol{u} \cdot \boldsymbol{\nabla} \omega = \nu \boldsymbol{\nabla}^2 \omega \tag{42}$$

The vorticity ω is computed at each time step in Fourier space. Then, each Fourier coefficient is gouverned by the following equation:

$$\frac{\partial \hat{\omega}_{\alpha\beta}}{\partial t} - T_{\hat{\omega}_{\alpha\beta}} = -\frac{(\alpha^2 + \beta^2)}{Re} \hat{\omega}_{\alpha\beta} \tag{43}$$

with

$$T_{\hat{\omega}_{\alpha\beta}} = -\imath \sum_{(\alpha_1,\beta_1)+(\alpha_2,\beta_2)=(\alpha,\beta)} \left(\alpha_2 \hat{u}_{\alpha_1\beta_1} + \beta_2 \hat{v}_{\alpha_1\beta_1}\right) \omega_{\alpha_2\beta_2} \tag{44}$$

The advection-diffusion equation for Θ is solved in the same way as the vorticity equation (both are similar). The vorticity, scalar and Lagrangian equations for particles

[4]Property code, CEMAGREF, Johan Carlier

$i = 1, N$ give the whole differential system:

$$\frac{\partial\left(\hat{\omega}_{\alpha\beta}\exp\frac{(\alpha^2+\beta^2)}{Re}t\right)}{\partial t} = T_{\hat{\omega}_{\alpha\beta}}\exp\frac{(\alpha^2+\beta^2)}{Re}t \quad (45)$$

$$\frac{\partial\left(\hat{\Theta}_{\alpha\beta}\exp\frac{(\alpha^2+\beta^2)}{Pe}t\right)}{\partial t} = T_{\hat{\Theta}_{\alpha\beta}}\exp\frac{(\alpha^2+\beta^2)}{Pe}t \quad (46)$$

$$\frac{dx_i}{dt} = u \quad (47)$$

$$\frac{dy_i}{dt} = v \quad (48)$$

The vorticity and scalar equations are solved in Fourier space using dealiased Fourier expansions in two directions with periodic boundary conditions. The time integration is third-order/three steps with a Runge-Kutta scheme. $T_{\hat{\omega}_{\alpha\beta}}$ is computed in physical space to reduce the computation time. The code is called pseudo-spectral.

x_i and y_i are solved in the physical space inside the vorticity equation computation using the same Runge-Kutta scheme in order to use the intermediate velocity components u and v determinated in $T_{\hat{\omega}_{\alpha\beta}}$. However, an interpolation (bicubic) of the velocity field has to be applied as the particles are not supposed to be located on the nodes of the grid.

For the Fluid project, sustaining turbulence along the time is of great interest to allow time averaging of statistical quantities in the post-processing, for evaluation purposes. Then, the vorticity equation is slighty modified:

$$\frac{\partial\hat{\omega}_{\alpha\beta}}{\partial t} - T_{\hat{\omega}_{\alpha\beta}} = -\frac{(\alpha^2+\beta^2+Re_\nu)}{Re}\hat{\omega}_{\alpha\beta} + f \quad (49)$$

where f is a forcing term proportional to the vorticity and random on the Fourier coefficients, and Re_ν a friction term adding only for the first modes. That results enstrophy injection dissipated by small scale with Re and energy injection dissipated by large scales with Re_ν (see figure 7).

3.2.2 Set of images delivered

Different sets of parameters have been tested. The strategy was to select the maximum number of nodes for a reasonable computation time with the computer available, the maximum Re and Pe for this grid size and a target Energy/Enstrophy injection which could be dissipated by the system. Finally, two sets of parameters were selected as summarized below:

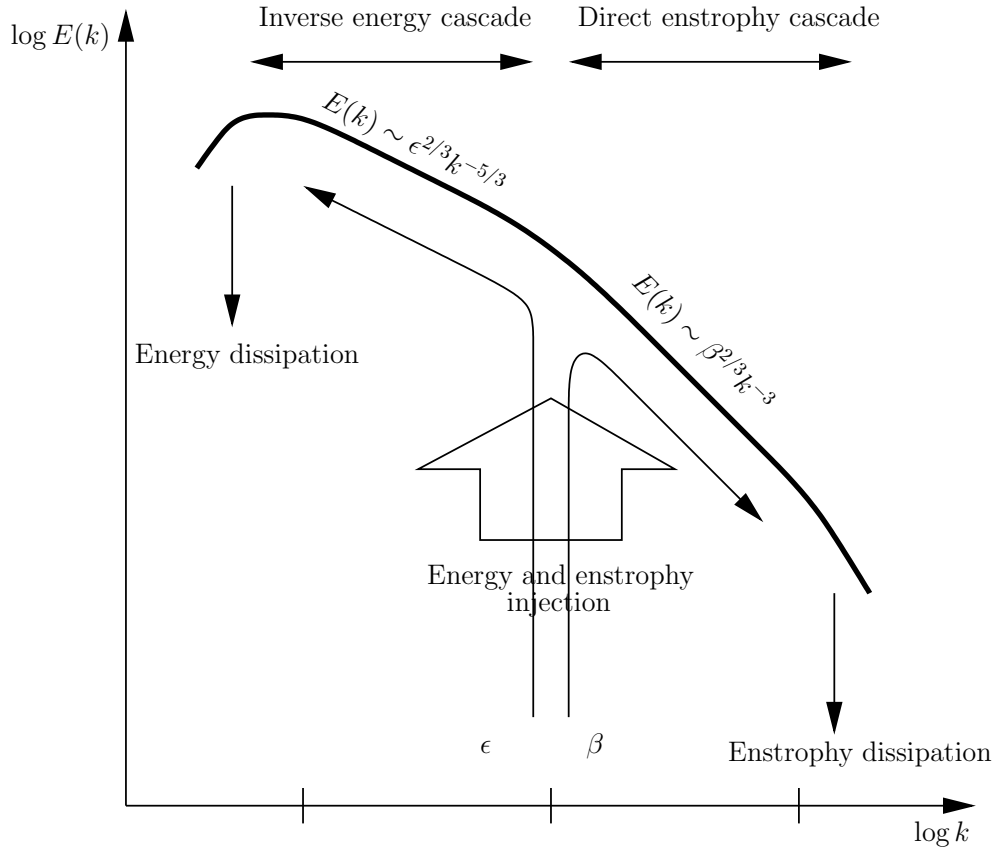

Figure 7: Energy and enstrophy cascade

Run	12	02
Number of nodes	$1\,024 \times 1\,024$	256×256
cfl	0.5	0.5
Re	30 000	3 000
Re_ν	5	5
Pe	no scalar	2 100
Sc	no scalar	0.7
Location of the initial maximum	40	40
Forcing band	$[5; 10]$	$[5; 10]$
Target enstrophy dissipation	0.1	0.1
Proportion of random/proportional forcing	0.5	0.5
Time step Δt	0.001	0.01
Size box	2π	2π

In run 12, only particles are transported. In run 02, both particles and scalar are transported.

In "package_02/dns_tur2d/run12/", "field/" contains the velocity and vorticity solutions ("run010200[000-199].uvo") and "particle/" the particle images (Case C2,"run010200[000-199].tif"). Then, the sequence consists of 200 successive images ($1\,024 \times 1\,024$ px^2) with a time separation $\Delta t = 0.001$.

In "package_02/dns_tur2d/run02/", "field/" contains the velocity and vorticity solutions ("run01005[000-999]0.uvo"), "particle/" the particle images (Case C1a, "run01005[000-999]0.tif") and "scalar/" the scalar images (Case C1b, "run01005[000-999]0.tif"). Then, the sequence consists of $1\,000$ successive images (256×256 px^2) with a time separation $10\Delta t = 0.1$.

Case n°	Description	Directory
B	Exp. of 2D turbulent flow	USB-HDD ./package_02/exp_turb2d/
C1a	DNS Turb 2D Time resolved	USB-HDD ./package_02/dns_turb2d/run02/particle/
C1b	DNS Turb 2D Time resolved	USB-HDD ./package_02/dns_turb2d/run02/scalar/
C2	DNS Turb 2D Time resolved	USB-HDD ./package_02/dns_turb2d/run12/

Table 5: Table location, Annexe A.3

Fig. 8 presents two samples of the scalar images and the corresponding particle images at different instant.

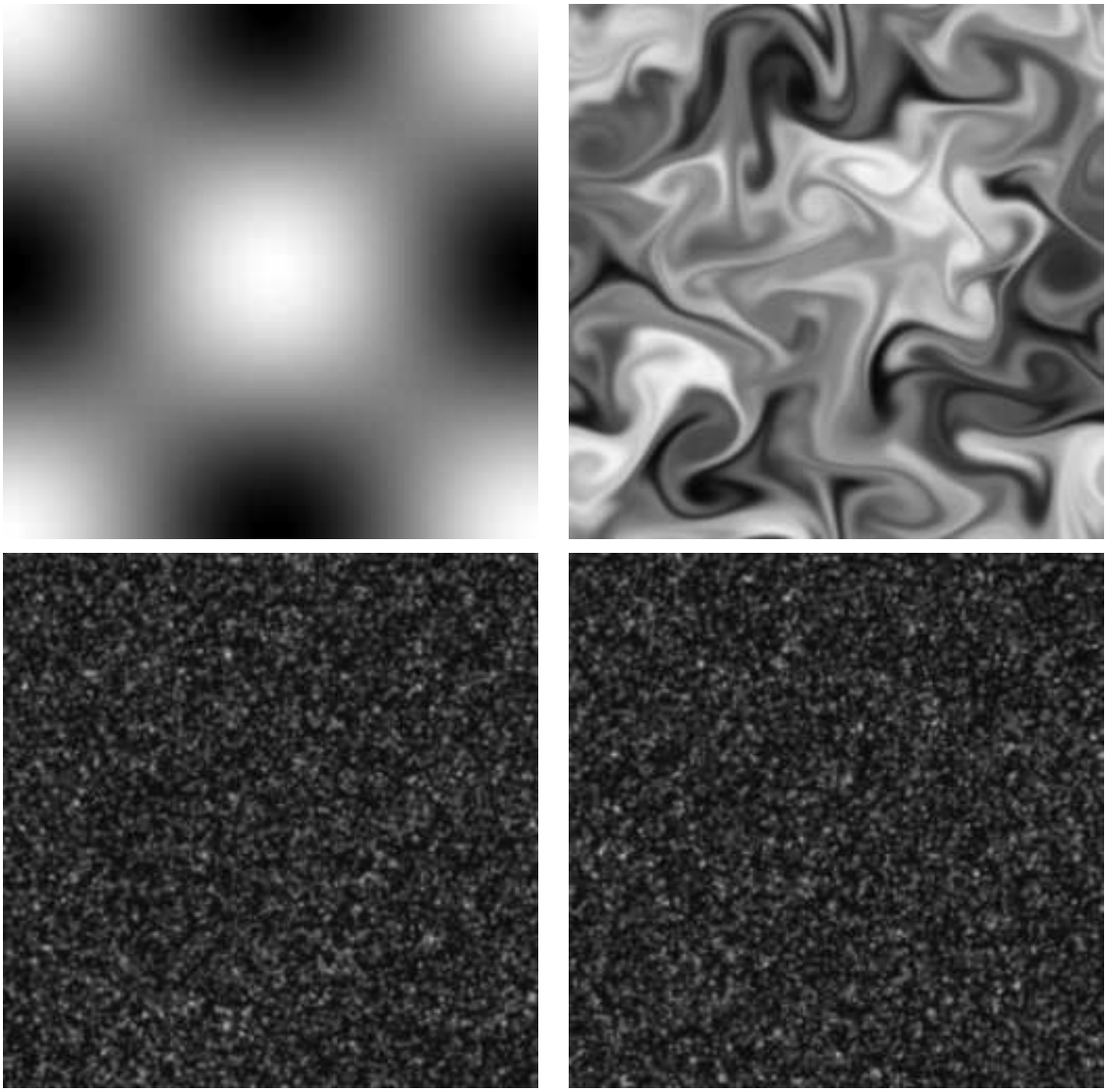

Figure 8: Two samples of the scalar images and the corresponding particle images

A Description of Synthetic images Generator

A.1 $2D$ image

An initial field of particles was generated with an uniform random distribution of the coordinates (x, y, z) in a $3D$ domain. The size of the domain is given in meter and pixel for the width and the height and only in meter for the thickness. The figure 9 presents the $3D$ domain containing the light sheet and the particles. The origin is located at the center of the domain.

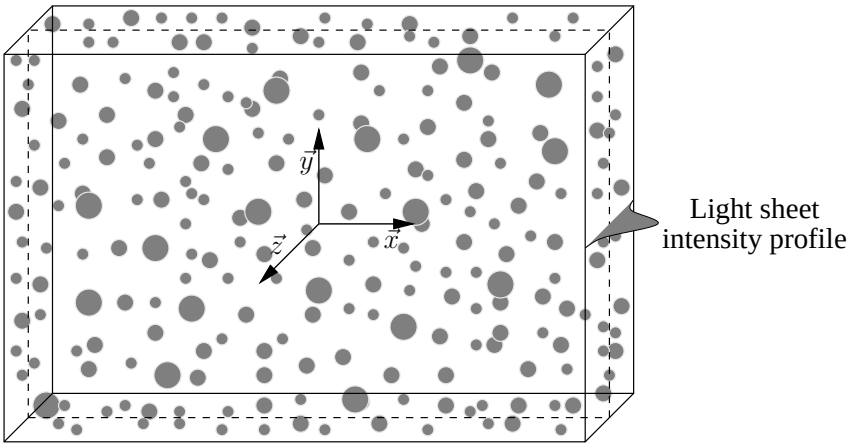

Figure 9: $3D$ domain containing light sheet and particles

The particle concentration is obtained through the choice of a fixed number of particles which are located in the domain by randomly assigning a (x, y, z) position to each particle. Each particle is given a diameter. The random distribution of this diameter is normal with a given mean value and standard deviation. Each particle image is given a shape using a $2D$ Gaussian repartition of the intensity over the neighbouring pixels of particle central position (x, y, z):

$$I^k(\vec{x}) = I(\vec{x}) \exp^{-\frac{1}{2}\frac{\left(x-x_0^k\right)^2+\left(y-y_0^k\right)^2}{D^{k2}}} \tag{50}$$

The peak intensity of each particle image depends on the position in the light sheet. In x and y direction, the light sheet intensity is constant. In z direction, it has a Gaussian profile centered on the median plane with maximum value of grey-levels q:

$$I(\vec{x}) = q \exp^{-\frac{1}{2}\left(\frac{4z}{\Delta z}\right)^2} \tag{51}$$

The thickness of the domain corresponds to 4 standard deviations for this Gaussian profile. Moreover, a constant background can be added.

In all the initial images, the particle image concentration was set homogeneous by fixing the number of particles in each window (the image was divided in windows). The concentration value was chosen very large in the case of gaussian profile in thickness because particles located far from the center of the laser sheet result 'not-visible' due to their very low intensity.

The digitalization was done by adding the contribution of the integration of each particle on the pixel:

$$I\left(x_i, y_i\right) = \sum_{k}^{N} I^k\left(x, y\right) \otimes \Pi\left(x, y\right) \otimes \delta\left(x - x_i, y - y_i\right) \tag{52}$$

where $\otimes$ is the convolution operator, Π the rectangular function and δ the Dirac function.

Lots of image parameters can be change as particle concentration, diameter, shape and quantification (grey level), and background noise can be added. Each field of particles was computed by applying a velocity field to the previous one, a time interval being adequaly chosen between the successive images. A $3D$ velocity field can be used to have particle disappearance for exemple.

A.2 $3D$ image

An initial field of particles was generated with an uniform random distribution of the coordinates (x, y, z) in a $3D$ domain. The 3 dimensions of the domain are given in meter and voxel.

The particle concentration is obtained through the choice of a fixed number of particles which are located in the domain by randomly assigning a (x, y, z) position to each particle. Each particle is given a diameter. The random distribution of this diameter is normal with a given mean value and standard deviation. Each particle image is given a shape using a $3D$ Gaussian repartition of the intensity over the neighbouring pixels of particle central position (x, y, z):

$$I^k\left(\vec{x}\right) = I\left(\vec{x}\right) \exp^{-\frac{1}{2}\frac{\left(x-x_0^k\right)^2+\left(y-y_0^k\right)^2+\left(z-z_0^k\right)^2}{D^k{}^2}} \tag{53}$$

The peak intensity of each particle image is constant:

$$I\left(\vec{x}\right) = q \tag{54}$$

The digitalization was done by adding the contribution of the integration of each particle on the pixel:

$$I\left(x_i, y_i, z_i\right) = \sum_{k}^{N} I^k\left(x, y, z\right) \otimes \Pi\left(x, y, z\right) \otimes \delta\left(x - x_i, y - y_i, z - z_i\right) \tag{55}$$

A.3 Database location

Case n°	Description	Directory
A1a	Poiseuille	FLUID-website ./WP01/package_01/
A2a	Lamb-Oseen vortex	FLUID-website ./WP01/package_01/
A3a	Uniform flow	FLUID-website ./WP01/package_01/
A4a	Sink flow	FLUID-website ./WP01/package_01/
A5a	Vortex flow	FLUID-website ./WP01/package_01/
A6a	Cylinder with circulation	FLUID-website ./WP01/package_01/
A1b	Poiseuille	USB-HDD ./package_02/analytic/
A2b	Lamb-Oseen vortex	USB-HDD ./package_02/analytic/
A3b	Uniform flow	USB-HDD ./package_02/analytic/
A4b	Sink flow	USB-HDD ./package_02/analytic/
A5b	Vortex flow	USB-HDD ./package_02/analytic/
A6b	Cylinder with circulation	USB-HDD ./package_02/analytic/
A7	single synthetic PIV image	FLUID-website ./WP01/package_04_LaVision/
B	Exp. of 2D turbulent flow	USB-HDD ./package_02/exp_turb2d/
C1a	DNS Turb 2D Time resolved	USB-HDD ./package_02/dns_turb2d/run02/particle/
C1b	DNS Turb 2D Time resolved	USB-HDD ./package_02/dns_turb2d/run02/scalar/
C2	DNS Turb 2D Time resolved	USB-HDD ./package_02/dns_turb2d/run12/
D1	Exp. far wake	USB-HDD ./package_02/exp_wake/
D2	*Exp. near wake*	
D3	*Exp. near wake - Time resolved*	
E1	LES wake - Volume	USB-HDD ./package_02/les_wake/
E2	*LES wake - Time resolved*	
F	real high-speed PIV images	FLUID-website ./WP01/package_03_LaVision/
G1	Volume - constant velocity	FLUID-website ./WP01/package_06_LaVision/
G2	Volume - compression wave	FLUID-website ./WP01/package_06_LaVision/
G3	Volume - comp. wave + gradient	FLUID-website ./WP01/package_06_LaVision/
G4	Volume - shear flow	FLUID-website ./WP01/package_06_LaVision/
G5	Volume - shear flow + gradient	FLUID-website ./WP01/package_06_LaVision/